NASA CR- 152589

(NASA-CR-152589) MRF STUDY. PART 2: ANTENNA DESIGN Final Report (Hughes Aircraft Co.) 86 p HC A05/MF A01 CSCL 09C

N77-32401

Unclas
G3/33 49299

FINAL REPORT OF MRF STUDY

PART II ANTENNA DESIGN

Contract No. NAS5-22468

February 1976

HUGHES
HUGHES AIRCRAFT COMPANY

CONTENTS

LIST OF ILLUSTRATIONS

1.0 INTRODUCTION

The primary thrust of the study effort devoted to the antenna subsystem of the Meteorological Radar Facility has been in the assessment of the practical feasibility of the design and construction of the antenna to meet the requirements of the conceptual radar system. Both the subscale antenna, nominally 5 by 4 meters in dimensions, and the full scale antenna, taken as nominally 18 by 4 meters in size, have been considered. The examination of feasibility has been from electrical, mechanical, and thermal standpoints. Fundamental, electrical, microwave design questions applying to both the subscale and the full-scale antennas have been considered in greater detail than questions of mechanical configuration and thermal design. The reason is twofold in that detailed mechanical and thermal analysis would be without significance were not electrical feasibility reasonably well established, and prior experience indicates that, at least in general, the mechanical and thermal difficulties can be expected to be surmountable with established techniques. Layouts have been made, however, in the development of preliminary configurations, along with a deployment method, for the subscale antenna in conjunction with the MMAP/EEE antenna cluster for alternate arrangements of the three-pallet configuration. Implementation of the array and support structure and attachment of the array to the support and thermal provision have been considered, but detailed mechanical and thermal analyses have been limited.

The study has provided resolution of certain essential questions of electrical feasibility relative to the microwave design of traveling-wave arrays for use in the antenna. The results show that a microwave design of antennas that incorporate traveling-wave arrays can be effected with the beam scanned to 45 degrees in elevation without occurrence of higher order beams,

i.e., grating lobes, in real space and that tolerance difficulties in fabrication can be minimized by the use of short, non-resonant, shunt slots as the radiating elements. In addition, although there are details of design to be determined and further analysis to be performed, there does not appear to be anything to prevent attainment of a feasible mechanical and thermal design. It must be emphasized that, although feasibility seems reasonably established, the effort necessary to complete the design, development, and test of a large complex electromechanical device of this nature is a protracted one. Although critical areas of electrical, mechanical, and thermal design can be designated, they are intimately interrelated in the design as a whole.

A preliminary design description considering some structural and deployment matters is given in the next section. Details of the treatment of questions of an electrical design and feasibility constitute Section 3. Section 4 treats antenna stabilization briefly, and the concluding section, number 5, contains a discussion of the matter of antenna specification.

2.0 DESIGN DESCRIPTION

The antenna as presently considered operates at X-band at a nominal frequency of 10 GHz. It consists of a narrow transmitting array less than 3 cm wide and a receiving antenna filling the remainder of the aperture, nominally 4 meters wide.

The receiving antenna consists of 185 parallel traveling-wave arrays that run the length of the antenna. Each traveling-wave array is a waveguide with shunt radiating slots in the broadwall of the guide. Approximately 330 slots are used in each 5-meter array and approximately 1200 in each 18-meter array. Since there are so many slots in each longitudinal array, the coupling of each slot to the waveguide is very low. To achieve and control this low coupling short, non-resonant, longitudinal, shunt slots are used. The slots are offset to one side of the centerline of the guide, and the coupling is controlled by both the offset and the slot length. The longitudinal slot spacing is approximately 0.600 inch. The traveling-wave arrays are placed side by side with a centerline-to-centerline spacing of 0.855 inch.

The transmitting antenna consists of one or two traveling-wave arrays like the receiving arrays described above and located parallel to them with a gap, possibly loaded, for isolation.

The maximum of each traveling-wave receiving pattern is situated on a conical surface that is at an angle of approximately 45 degrees from a plane perpendicular to the axis of the array. The response of the combination of 185 arrays in azimuth to provide multiple beams on the cone is not determined in the antenna itself. Rather, each longitudinal array provides an input to an indivudal receiver and the desired patterns in azimuth, 86 in number, are generated in the system processor by means of the

digitized received signals. The angle at which the "elevation" pattern maximum occurs is controlled by the wave velocity in the radiating guide, which is determined by the waveguide dimensions. The sidelobe level in that direction is controlled by the coupling of the slots, i.e., by the slot lengths and offsets.

The microwave portion of the antenna is supported by a thermally isolated structural assembly that also provides attachment points that remain co-planar to close tolerances (see Figure 2-1). The radiating arrays are arranged in panels or modules that must be structurally supported at intervals because of vibration, acoustic, and shock loads during launch, boost, and landing. It is anticipated that the thermally coated surface of the antenna will be exposed to the environment and that variations in the bulk temperature will cause expansion and contraction, as well as small thermal gradients from front-to-back of the array panels. As a result, the surfaces will tend to curve. To permit expansion and contraction, narrow gaps are provided at intervals in both directions. The result is expected to be one or two very small grating lobes, probably 25 dB or more down, near the edge of the main beam. To limit the departure from flatness due to thermal effects and to provide adequate support, the attach points, which permit small motions of the radiating panels relative to the backup structure in a parallel plane, need to be spaced, from preliminary estimates, at intervals of one to two meters. The exact distance will need to be determined in the course of detailed structural and thermal analysis. The planned attachments are combinations of thermal blocks and ball-spline supports.

The receivers and processing equipment mounted on the antenna structure are thermally isolated from the waveguide arrays. Short sections of waveguide of low thermal conductance deliver the array output signals to the receivers. Couplers are provided for the injection of calibration signals between the thermal blocks and receivers.

The matters of stowage and deployment of the antenna assembly have been considered in detail only for the 4x5-meter antenna. It has been assumed that the stowage is on a 3-pallet train, together with the MMAP/EEE antenna cluster, and that deployment takes place from this configuration. Three such configurations have been considered. The case in which a single

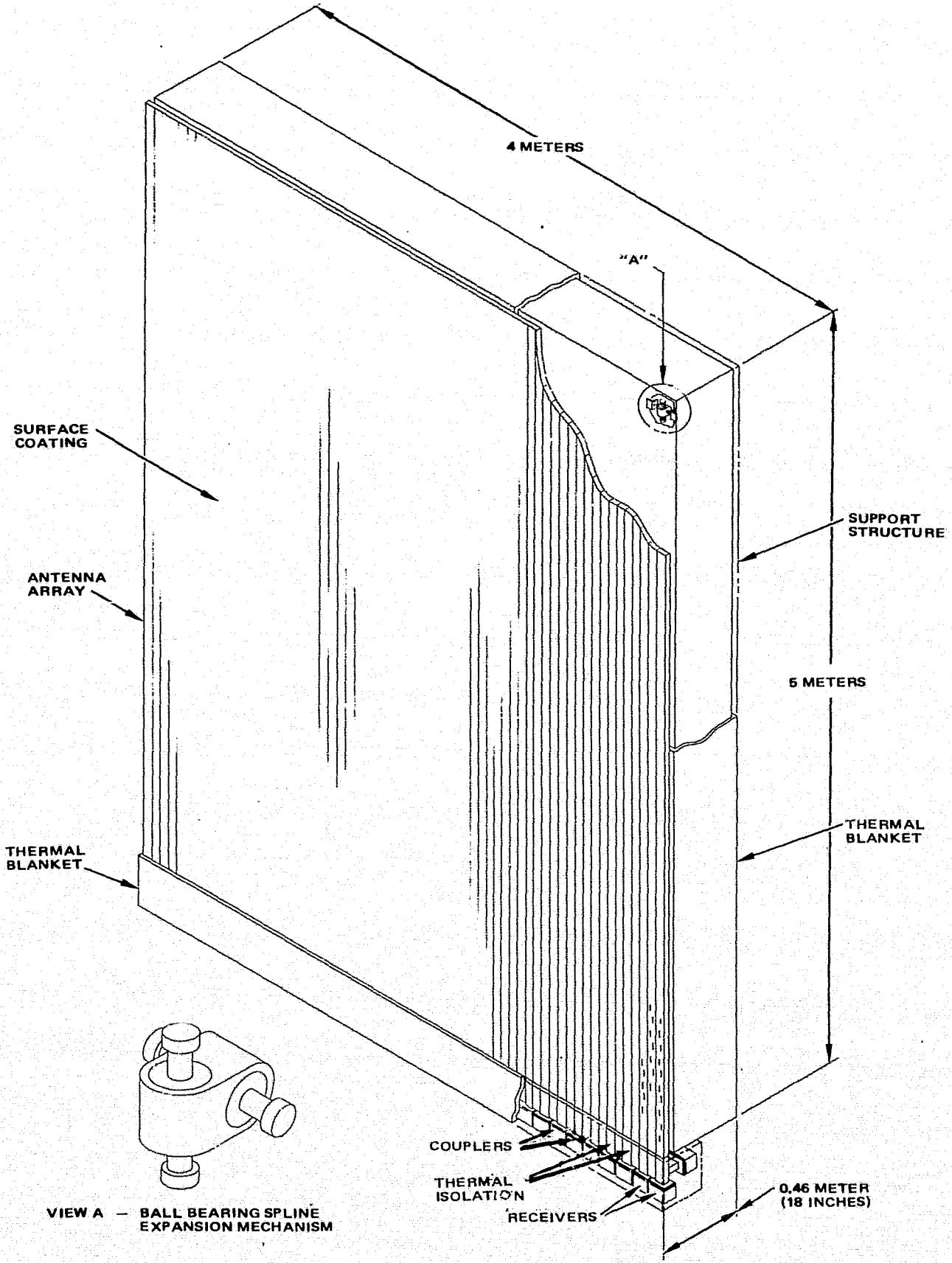

Figure 2-1 Antenna Schematic

4x5-meter antenna and the MMAP/EEE antenna cluster are mounted separately is illustrated in the deployed state in Figure 2-2; the corresponding stowage arrangement is shown in the layout of Figure 2-3. In this configuration the 4x5-meter antenna is deployed from the shuttle by erection into a vertical position: it is first rotated about an axis parallel to the leading horizontal edge and then rotated through 45 degrees about a vertical axis near one edge while the other edge is driven along a track. Erection and rotation are effected by means of ball-spline drives which are actuated by electric motors and locked by brakes in the unstablized arrangement. Restowage is effected in the reverse order from deployment. The time required for deployment or restowage is largely a question of the power rating of the deployment and restowage motors. Either process could easily be accomplished in 5 minutes. A design for the jettisoning mechanism has not been carried out, but preliminary consideration indicate that a simple, electrically actuated, spring mechanism with jettisoning guides should be reliable and effective.

The probable requirement for stabilization relative to a vertical or near vertical axis is indicated in Section 4. The same low-friction screws as used for the deployment, acting essentially as tangent screws, appear to be suitable for the small-angle motions needed. They can easily be provided with a servo drive. This sort of mechanism has been employed previously by Hughes in pointing controls for large space structures and has proved to be a reliable mechanization. A third axis would be needed for full three-axis control, but the implementation appears straightforward.

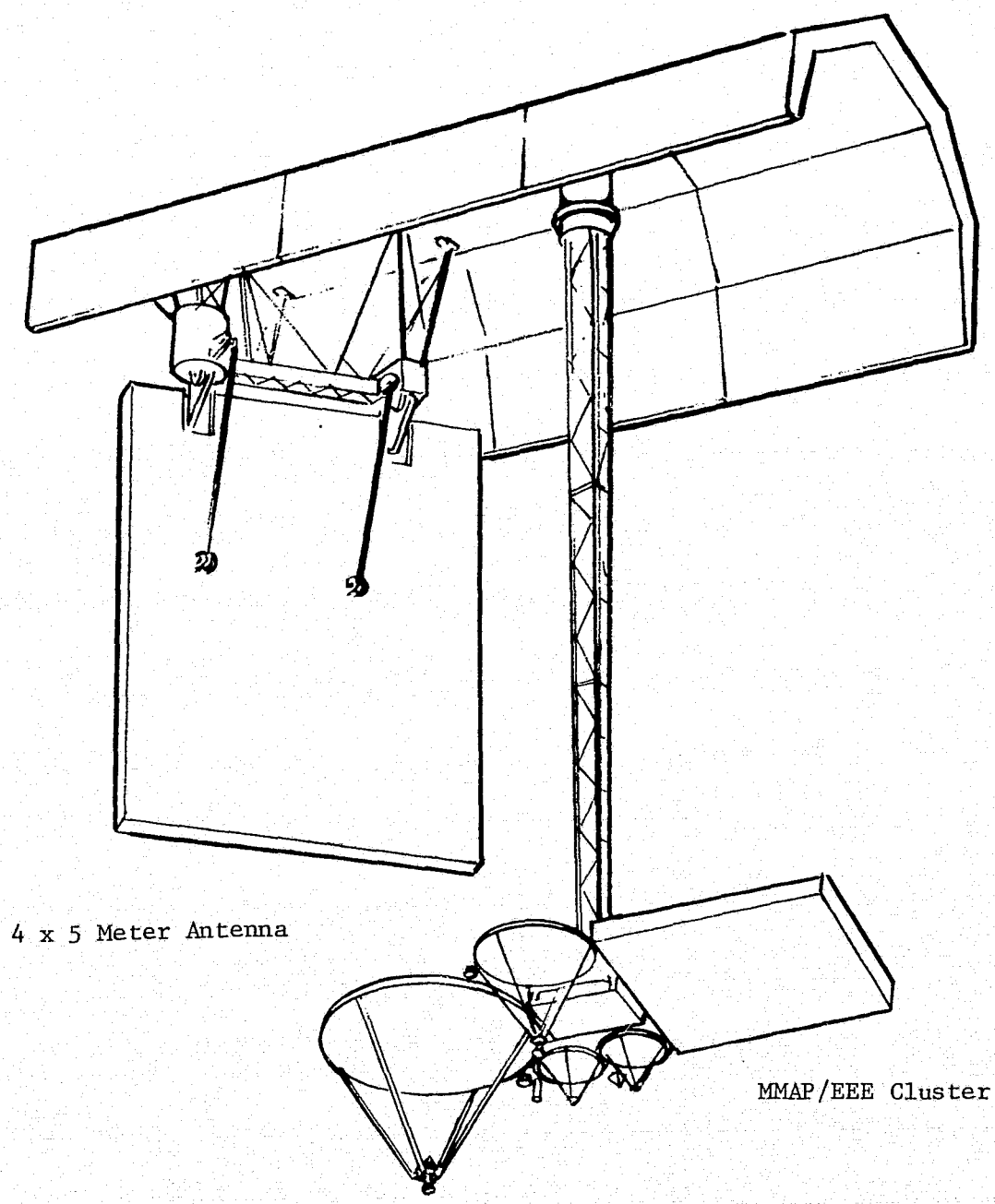

Figure 2-2 MRF Antenna Deployed from 3-Pallet Train

FOLDOUT FRAME

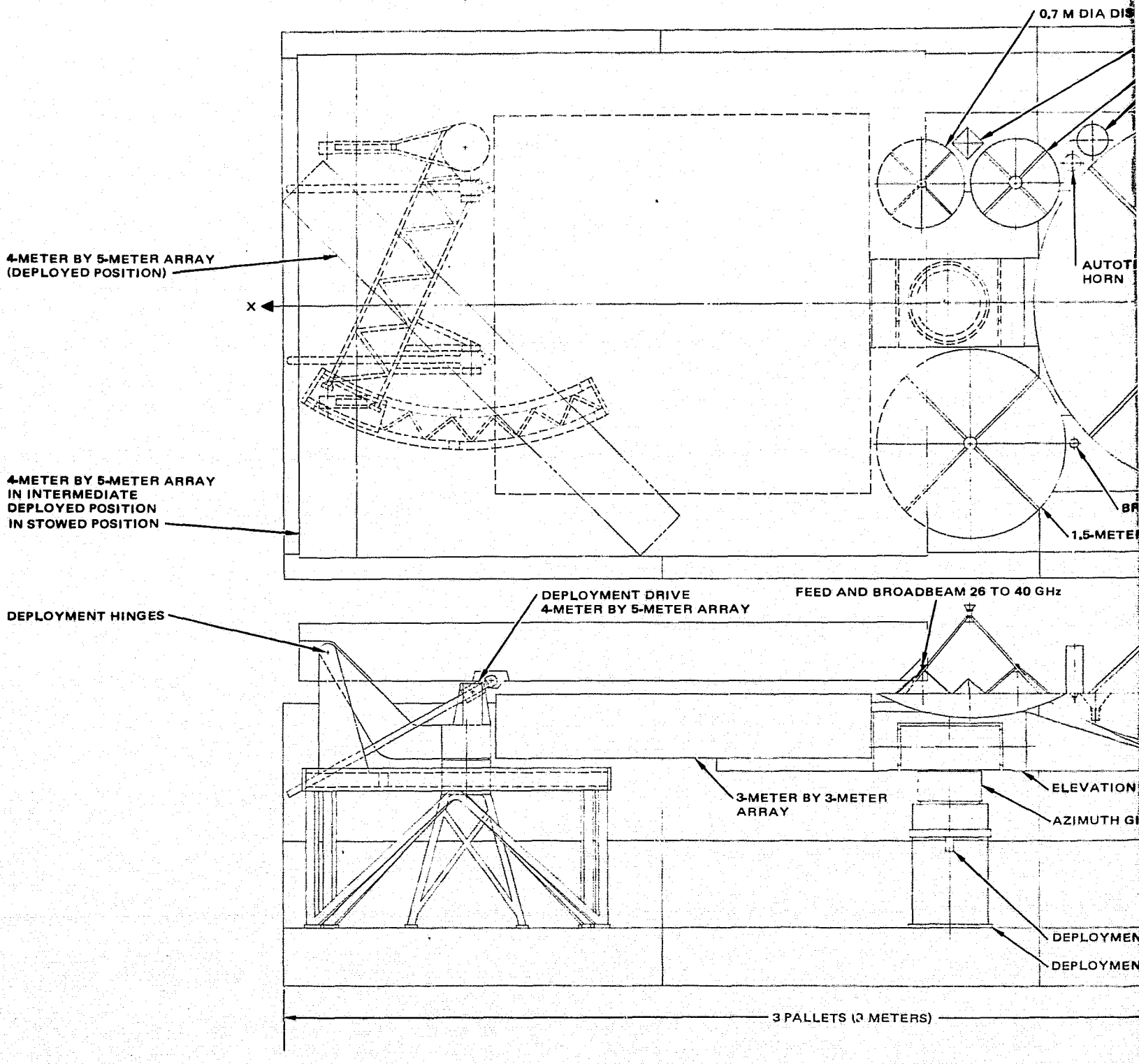

FOLDOUT FRAME 2

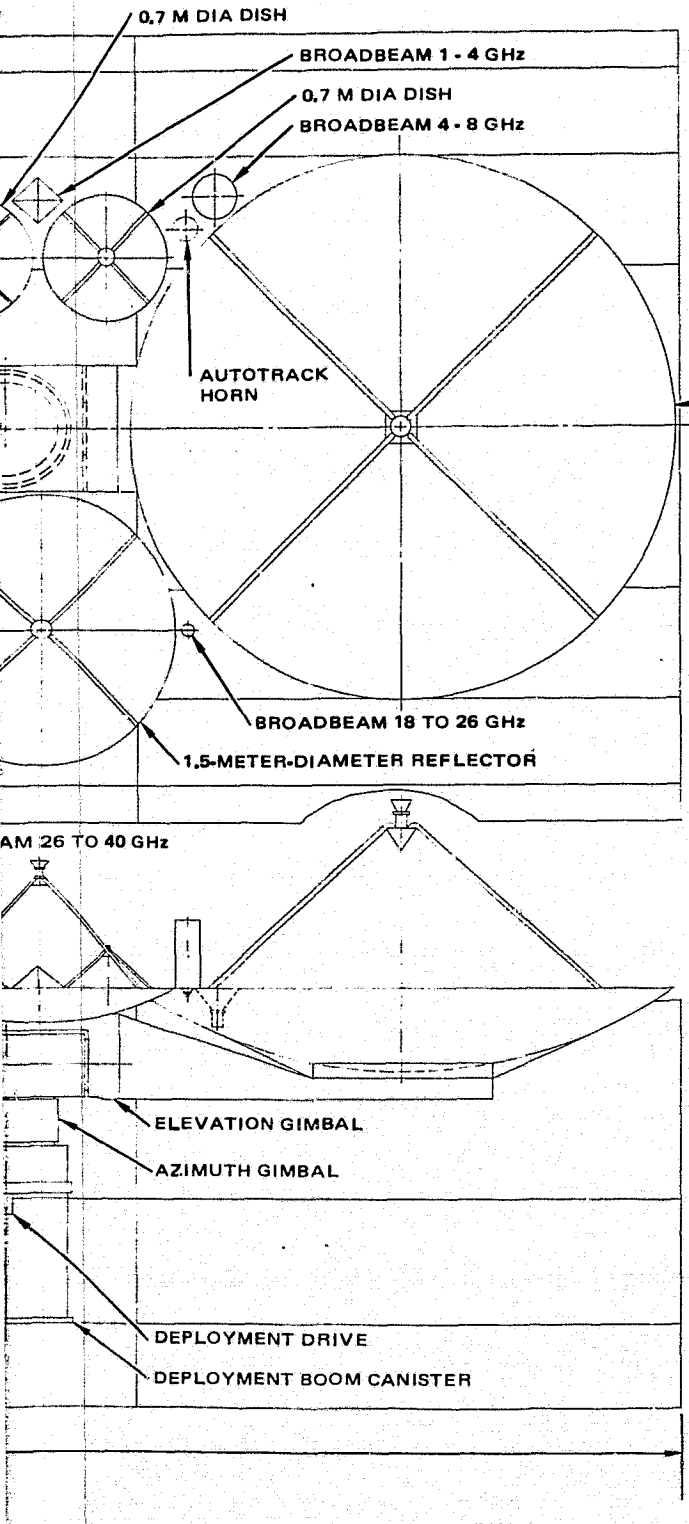

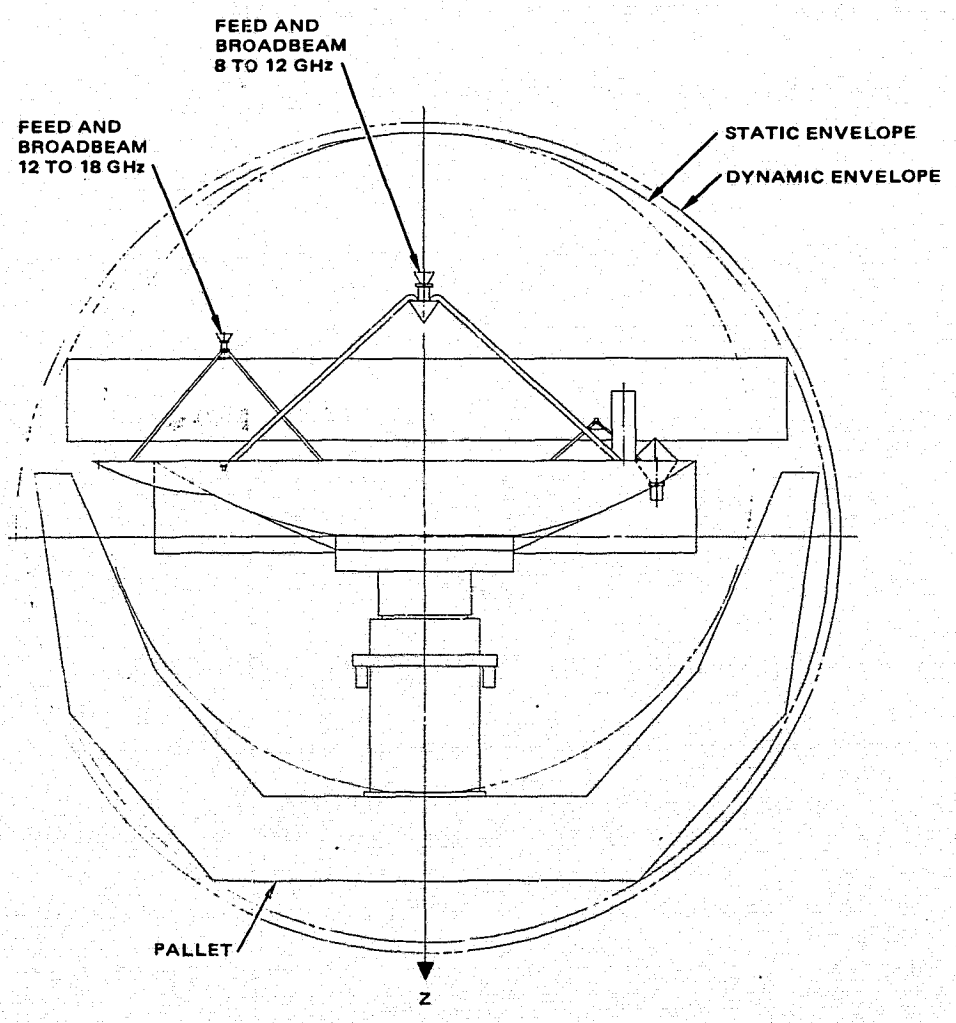

Figure 2-3. Layout of separate mount configuration.

3.0 ELECTRICAL DESIGN CONSIDERATIONS

The antenna subsystem should produce a transmitted beam that is narrow in elevation, with relatively low sidelobes, and that provides broad azimuthal coverage. The receiving pattern of the system should exhibit narrow beams and low sidelobes in both elevation and azimuthal directions.

For both transmitting and receiving modes, the antenna main beam must be scanned away from broadside in elevation about 45 degrees. Both beams must be scanned by the same amount. Only a portion of the overall aperture width, however, a narrow linear source, is used to produce wide azimuthal illumination for transmission.

On reception, the full aperture must be used to produce narrow azimuth coverage, and a multiple beam-forming mechanism must be provided. This mechanism takes the form of appropriate digital processing of the signals from individual linear arrays.

3.1 TRANSMISSION MODE

The field pattern of a single line source of identical radiating elements arrayed along the y-axis of a spherical coordinate system can be described by the equation

$$E(\theta, \phi) = \text{E.F. } (\theta, \phi) \sum_{i=1}^{N} A_i \, e^{j(i-1)\,[kd_y \sin\theta \sin\phi \; + \psi_y]} \qquad (1)$$

where θ and ϕ are coordinate angles defined in Figure 3-1, k is the wave number, d_y is the interelement spacing, ψ_y is the interelement progressive phase shift, E.F. (θ, ϕ) describes the radiation from a single element, and A_i is the excitation amplitude of the i^{th} element. For a main beam to be formed at, say,

$$\theta = 45°, \ \phi = 90°$$

$$\psi_y = -\frac{\sqrt{2}}{2} kd_y$$

and

$$kd_y \sin\theta \sin\phi + \psi_y = kd_y \left(\sin\theta \sin\phi - \frac{\sqrt{2}}{2} \right)$$

The contributions to the field of all elements of the array will then add in-phase when

$$\sin\theta \sin\phi = \text{constant}$$

This relationship describes a circle on any plane normal to the y-axis. A linear array of radiating elements thus exhibits a peak in the radiation pattern on a cone defined by the selected scan angle. A single linear array from the MRF aperture, or more than one as long as they are excited in-phase, can be made to illuminate only the required circle when transmitting. It is assumed that extraneous main beams, i.e., grating lobes, are inhibited by suitable dimensioning of the array. This subject is pursued more carefully in succeeding sections.

As a point of reference, it is worth noting that approximately 800 phase shifters, housed in a corporate feed network, would be necessary to scan the transmitting main beam if each radiating element were fed independently.

3.2 RECEIVING MODE

In the receiving mode, all the linear arrays that comprise the full aperture are used, approximately 185. Each must be scanned off broadside in elevation to the same pointing direction as that employed on transmission. Independent feeding of each radiating element would then imply that approximately 160,000 microwave phase shifters must be used (along with complex corporate feeds). Alternatively, 160,000 digital processor inputs could be employed. In any event, the complexity associated with independently fed radiating elements is overwhelming. It appears that this situation may be

avoided by the employment of slotted waveguide line sources. These are traveling-wave devices and, conceptually, can be made to scan in elevation without phase-shifting or signal processing complexity.

3.3 SCAN ANGLE RELATIONSHIPS AND THE TRAVELING WAVE ARRAY (RECEIVING MODE)

Figure 3-1 shows a planar aperture constructed from M identical traveling-wave, linear, slot arrays. Each linear array houses N radiating slots which, for the purpose of discussion, may or may not be positioned on alternate sides of the waveguide centerline. All the arrays are assumed to be fed independently from sources that can be phase-shifted so that scanning occurs between the limits of ± 35 degrees in γ. In addition, the main beam must be scanned to approximately $\theta = 45$ degrees. A rectangular slot lattice is assumed.

The electric field from a single traveling-wave slot array terminated by a matched load can be described by one of two equations. First, for an array in which consecutive slots are staggered, i.e., positioned, on opposite sides of the waveguide centerline,

$$E(\theta) = \sum_{i=1}^{N} A_i e^{j\,(i-1)\,[kd_y \sin\theta - \beta d_y + \pi]}$$

where $k = 2\pi/\lambda_o$, $\beta = 2\pi/\lambda_g$, d_y = slot spacing, λ_o = free space wavelength, and λ_g = wavelength in the guide.

When non-staggered slots are used, the equation becomes

$$E(\theta) = \sum_{i=1}^{N} A_i e^{j\,(i-1)\,[kd_y \sin\theta - \beta d_y]}$$

Different beam-scan conditions hold for these two situations. For the staggered and non-staggered cases, respectively,

$$\sin\theta_s = \lambda_o/\lambda_g - \lambda_o/2d_y \qquad (2)$$

$$\sin\theta_s = \lambda_o/\lambda_g \qquad (3)$$

Equations (2) and (3) can be cast into the forms

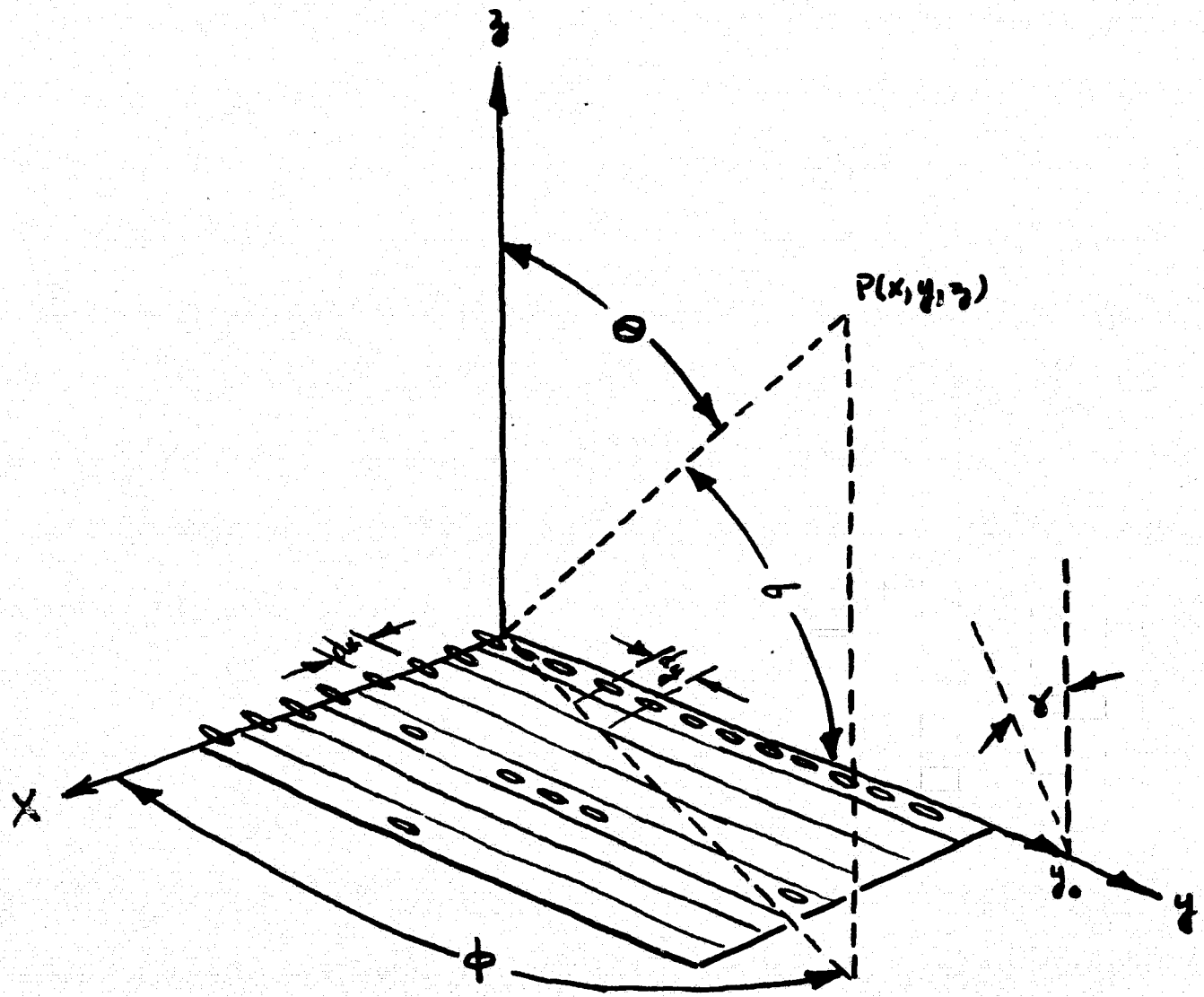

MRF PLANAR ARRAY IN COORDINATE SYSTEM

FIGURE 3-1

$$\sin \theta_s = [1 - (1/X)^2]^{1/2} - \frac{.5}{(d_y/\lambda_c)\ X} \tag{4}$$

where λ_c is the cutoff wavelength of the waveguide and

$$\sin \theta_s = [1 - (1/X)^2]^{1/2} \tag{5}$$

where

$X = f/f_c$, f is the frequency, and f_c the cutoff frequency for the guide.

The scan angle from these equations may then be plotted versus f/f_c with d_y/λ_c as a parameter. Note that equation (5) is independent of d_y, the element spacing in the y direction. Alternately, equation (4) can be expressed as

$$\sin \theta_s = [1 - (1/X)^2]^{1/2} - \frac{0.5}{d_y/\lambda_o} \tag{6}$$

and the angle plotted with d_y/λ_o as a parameter. Such a plot is presented in Figure 3-2. Propagation of only the dominant mode is implicit in this construction. Some interesting observations are possible with reference to Figure 3-2. First, staggered slots are most effective for small beam-scanning applications. A wide range of reasonable choices is possible for θ_s less than 5 degrees. There is flexibility in scanning the beam either toward or away from the input port. However, as the required scan angle increases a staggered slot geometry results in one of two undesirable conditions: either the array must be operated near cutoff with beam scan toward the input port, or a large d_y/λ_o must be tolerated with beam scan away from the input port. In the latter case, operation farther from cutoff is possible. However, effects from extraneous main (second-order) beams are likely to be substantial. For the MRF antenna, the former mode of operation could probably be made to produce a beam scan of 45 degrees. An implication of this choice would be a need for compromise among factors such as loss, extraneous main beams, waveguide dimensions, and far-end feeding details.

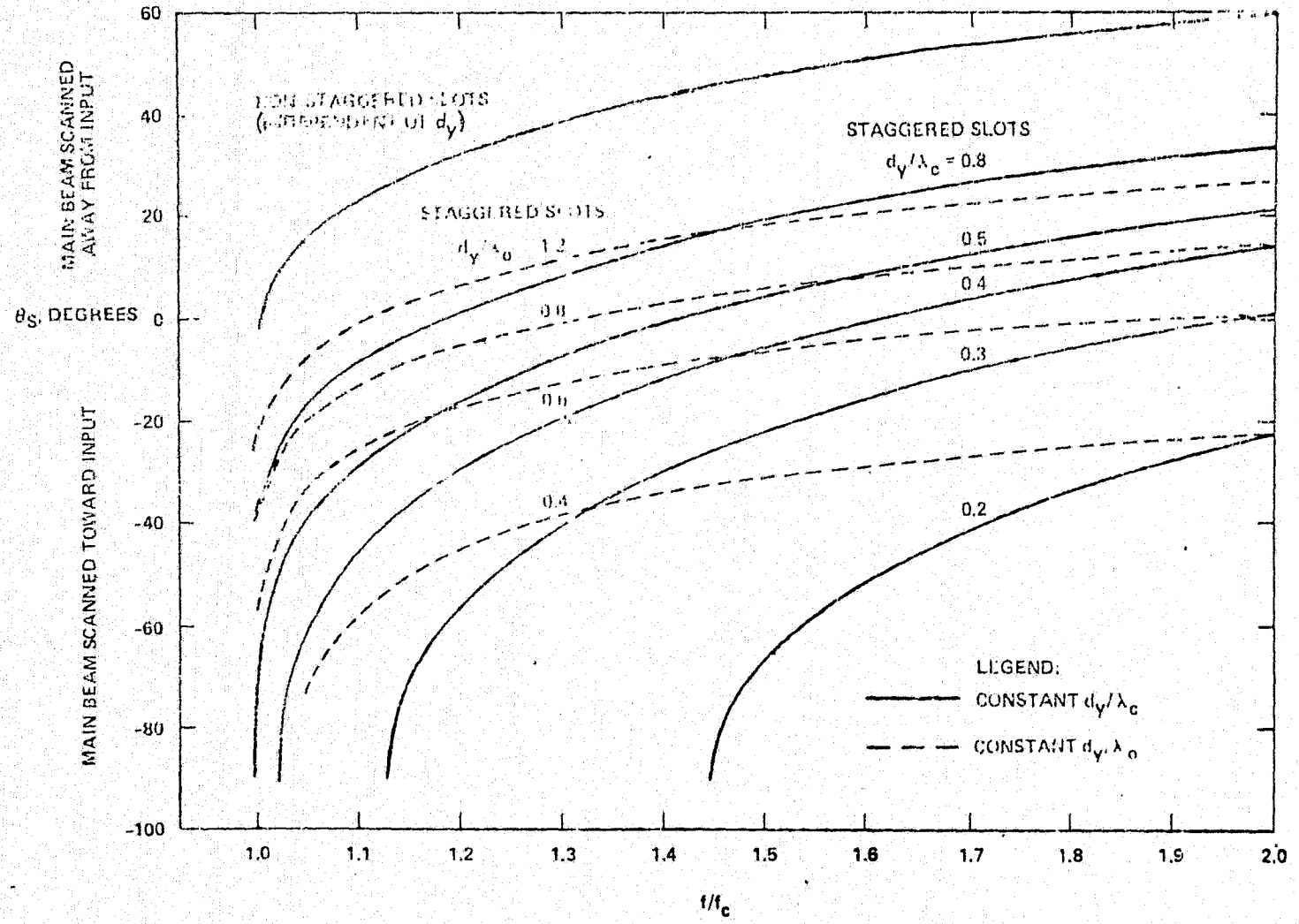

Figure 3-2. Traveling Wave Slot Array Scan Angle Relationships

Under no reasonable circumstances does it appear desirable to scan 45 degrees away from broadside with staggered slots.

If all radiating slots in the linear array are positioned on the same side of the waveguide centerline, Figure 3-2 indicates that a 40- to 50-degree beamscan away from the input port is possible without explicit penalty. Of course, the effects of extraneous main beams must still be checked independently. When non-staggered slots are used, the interelement phase shift is $\psi_y = -\beta d_y$. In keeping with these facts, the non-staggered traveling-wave slot array has been chosen as a suitable candidate for the MRF array.

3.4 GRATING LOBE SUPPRESSION

Scan angle relationships and grating lobe information can be examined by consideration of the aperture array factor and grating lobe diagrams. For this array of slot radiators, the array factor, A.F.(θ, ϕ), can be written

$$A.F.(\theta, \phi) = \sum_{i=1}^{M} \sum_{m=1}^{N} A_{im}\, e^{j(i-1)\,[kd_x \sin\theta \cos\phi + \psi_x]} \cdot e^{j(m-1)\,[kd_y \sin\theta \sin\phi + \psi_y]}$$

An equally useful description of this periodic aperture can be written in terms of Floquet modes:

$$A.F.(\theta, \phi) = \sum_{p=o}^{\infty} \sum_{q=o}^{\infty} A_{pq}\, e^{jk_{x_p} x}\, e^{jk_{y_q} y}\, e^{-j\Gamma_{pq} z}$$

$$k_{x_p} = \frac{2\pi p - \psi_x}{d_x}; \quad k_{y_q} = \frac{2\pi q - \psi_y}{d_y}$$

$$\Gamma_{pq}^2 = k^2 - \left[\frac{2\pi p - \psi_x}{d_x}\right]^2 - \left[\frac{2\pi q - \psi_y}{d_y}\right]^2$$

The Floquet mode description is a convenient tool for examination of grating lobe (second-order beam) behavior. Grating lobes are main beams,

other than the principal main beam, that may exist in visible θ, ϕ space. Their existence depends on the periodicity (d_x and d_y) of the structure and on the phasing (ψ_x and ψ_y) necessary to steer the principal beam. In general, it is desirable that the grating lobes be maintained well outside visible space; otherwise their presence can seriously reduce the gain in the direction of the principal beam by the diversion of energy and can introduce unwanted signals into the system. Even an incipient, or grazing, grating lobe can result in serious aperture mismatch effects.

From the Floquet description,

$$\Gamma_{pq} = k\left\{1-\left[\frac{p\lambda o}{d_x} - T_x\right]^2 - \left[\frac{q\lambda o}{d_y} - T_y\right]^2\right\}^{1/2}$$

where ($T_x = \sin\theta\cos\phi$) and ($T_y = \sin\theta\sin\phi$) are the direction cosines for the direction of pointing of the principal beam, with interelement phase shifts ψ_x and ψ_y, respectively. Γ_{pq} is real for a mode that propagates throughout space and imaginary for a mode that attenuates away from the aperture. Ideally, only the p=q=0 mode should propagate, with all others damped.

Those critical dimensions that allow higher order Floquet modes to propagate can be found by setting $\Gamma_{pq} = 0$:

$$T_{xp}^2 + T_{yq}^2 = 1$$

where

$$T_{xp} = \frac{p\lambda o}{d_x} - T_x \text{ and } T_{yq} = \frac{q\lambda o}{d_y} - T_y$$

From these relationships the critical array dimensions that allow grazing incidence of the $(p,q)^{th}$ Floquet mode can be found. For the case at hand, certain constraints can be imposed with respect to the direction cosines for the principal beam, T_x and T_y.

$$kd_y T_y = kd_y \sin\theta \sin\phi = -\psi_y = \beta d_y$$

$$T_y = \sin\theta \sin\phi = \frac{\lambda_o}{\lambda_g}$$

With reference to Figure 3-1, $\sin\theta \sin\phi = \cos\sigma$. Since it is desired that $\sigma \simeq 45$ degrees, $\sin\theta \sin\phi = \frac{\sqrt{2}}{2} = T_y$. This also constrains the broad dimension of all traveling-wave arrays because

$$\frac{\lambda_o}{\lambda_g} = \frac{\sqrt{2}}{2} \qquad a_{wg} = \frac{\lambda_o}{\sqrt{2}} \simeq 0.835 \text{ inch}$$

Thus, if a waveguide wall of 0.020 inch is assumed, $d_x = 0.855$ inch. Furthermore,

$$T_x^2 + T_y^2 = \sin^2\theta \; ; \quad T_x^2 = 0.5 - \cos^2\theta$$

Again with reference to Figure 3-1,

$$\tan\gamma = \frac{x}{z} = \frac{\sin\theta \cos\phi}{\cos\theta} = \frac{T_x}{\cos\theta}$$

Substitution yields

$$T_x^2 = 0.5 - \frac{T_x^2}{\tan^2\gamma}$$

Then

$$T_x = \sin\theta \cos\phi = \left(\frac{\sqrt{2}}{2}\right) \sin\gamma$$

and finally,

$$\left[\frac{p\lambda o}{0.855} - \left(\frac{\sqrt{2}}{2}\right) \sin\gamma\right]^2 + \left[\frac{q\lambda o}{d_y} - \frac{\sqrt{2}}{2}\right]^2 = 1$$

Rearranging terms and solving for d_y gives

$$d_y = \frac{1.18029\ q}{\left\{1 - \left[1.380456p - \frac{\sqrt{2}}{2} \sin\gamma\right]^2\right\}^{1/2} + \frac{\sqrt{2}}{2}}$$

From the preceding expression it can be shown that the (0, 1) mode is grazing for $d_y = 0.691$ and $\gamma = 0$. This mode then moves into invisible space as γ is scanned either positive or negative. The (-1, 1) mode becomes grazing for $\gamma = -35$ degrees, and the (1, 1) mode grazes for $\gamma = +35$ degrees. In both cases the change occurs for $d_y = 1.269$. However, in this event, the (0, 1) mode always propagates. Figure 3-3 shows a grating lobe diagram with these modes in the $T_x - T_y$ plane with $d_x = 0.855$ inch and $d_y = 0.691$ inch. The equation for each higher order Floquet mode is a displaced unit circle in the $T_x - T_y$ plane, while the unit circle centered at the origin delineates visible and invisible space for the principal (0, 0) mode. This figure shows that mode (0, 1) is just grazing for $\gamma = 0$ and cannot propagate for $\gamma \neq 0$. The (-1, 1) and (1, 1) modes are also non-propagating. Figure 3-4 is a grating lobe diagram in which $d_x = 0.855$ inch and $d_y = 1.269$ inches. With the latter dimensions, the (0, 0) and (0, 1) modes propagate for all values of T_x. Modes (-1, 1) and (1, 1) are grazing at the T_x scan limits. Note that, in both Figures 3-3 and 3-4, the (1, 0) and (-1, 0) modes are positioned identically. They depend only on d_x.

Results of this exercise show that array dimensions can be selected to satisfy principal mode scan requirements and, at the same time, avoid grating lobe incidence. To do this d_x must be set at approximately 0.855 inch, and slot spacing in the linear arrays must be kept well below 0.691 inch. These are reasonable numbers with which to work.

3.5 MAIN BEAM SCAN VERSUS FREQUENCY

T_x and T_y, the principal Floquet mode expressions, can be used to illustrate the movement of the main beam as the frequency is changed.

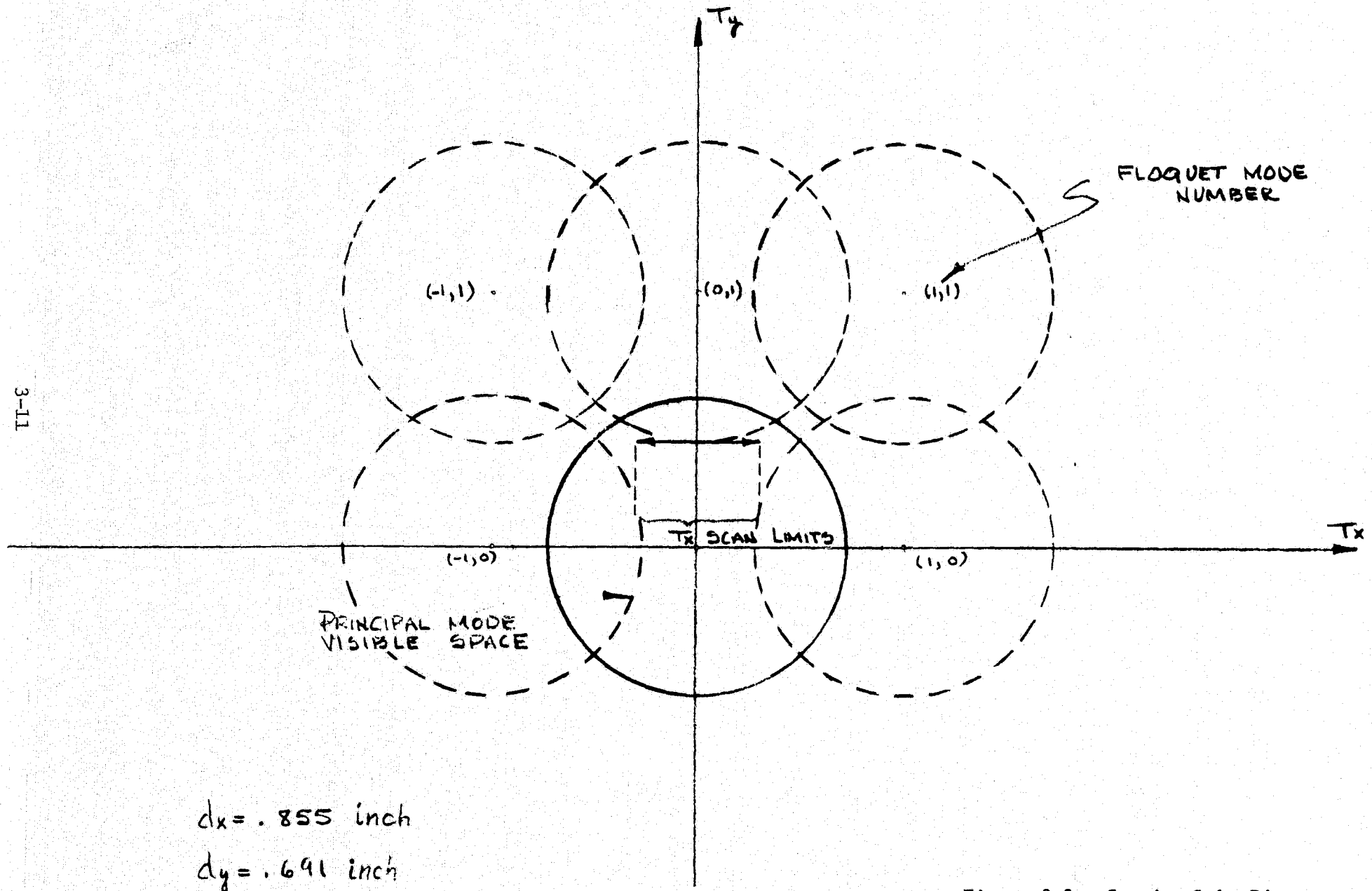

Figure 3-3. Grating Lobe Diagram

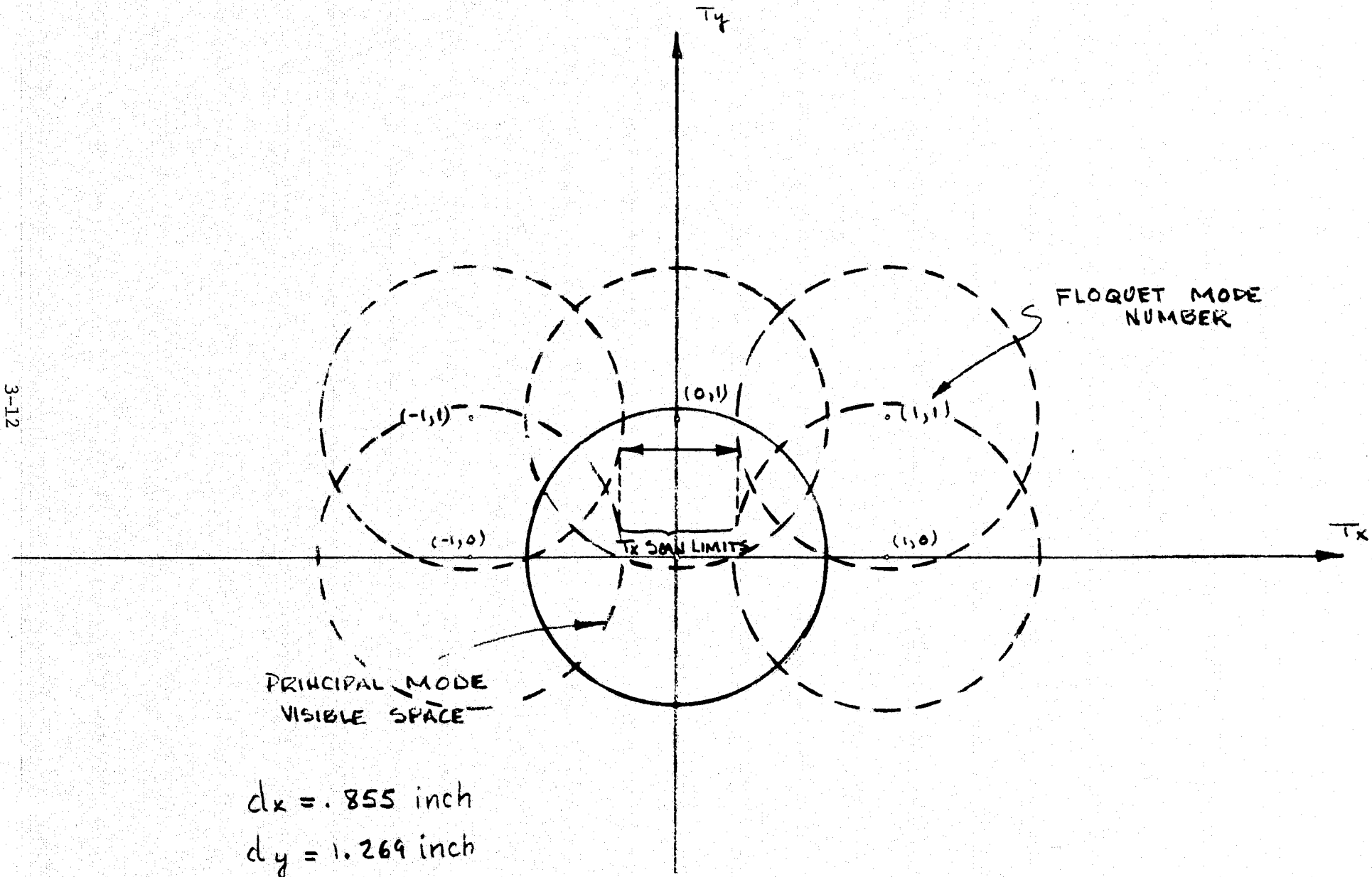

Figure 3-4. Grating Lobe Diagram

$$T_y\ (0,0) = \frac{\lambda_o}{\lambda_g} - \cos\sigma \tag{7}$$

$$T_x^2\ (0,0) = 1 - \cos^2\theta - \cos^2\sigma = \psi_x \frac{\lambda_o}{2\pi d_x}$$

But

$$\cos\theta = \frac{T_x}{\tan\gamma}$$

so that

$$T_x = \psi_x \frac{\lambda_o}{2\pi d_x} = \sin\sigma \sin\gamma$$

and, since σ and d_x are not independent,

$$\sin\gamma = \psi_x \frac{a}{\pi d_x} \tag{8}$$

where d_x = a + waveguide wall thickness.

Clearly, σ is frequency dependent and γ is not. At 10 GHz, a planar array 4.3 meters by 18 meters, scanned 45 degrees in elevation, will have an elevation beamwidth of approxiamtely 0.18 degree. The σ beam position shift normalized to this beamwidth, is an important system consideration. Figure 3-5 gives this information.

The fact that γ is frequency independent results uniquely because σ is independent of d_y. Another interesting feature of this type of array is that, for γ = 90 degrees, $\psi_x \simeq 180$ degrees. This relation is literally true for zero waveguide wall thickness and holds regardless of the σ value selected, as is demonstrated in the Appendix.

3.6 THEORETICAL SLOT CONDUCTANCE

It is anticipated that different phases of the MRF program will require array lengths of 5 meters and 18 meters. Because both are quite long at 10 GHz, a large number of radiating slots will be needed for each.

Figure 3-5. Normalized β Beamshift vs. Frequency

Waveguide Broad Dimension =0.835 inch

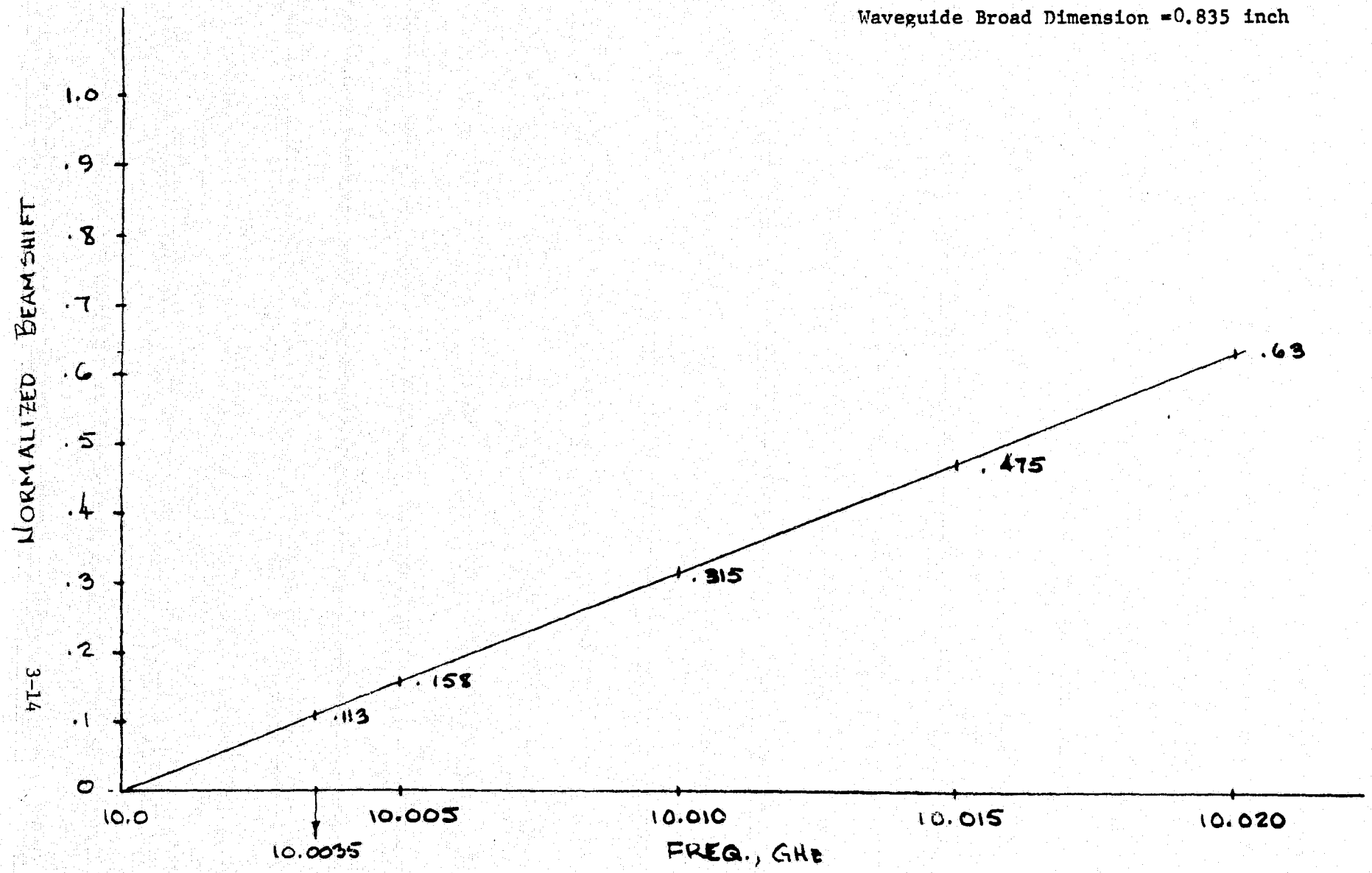

Each 5-meter linear array will house approximately 330 slots, while the 18-meter version will require approxiamtely 1200.

Very long traveling-wave arrays such as these can pose a number of unusual problems. Probably the most serious among these surrounds the fact that very small conductance values are needed. Every problem is unique, however, and in order to view the MRF situation, it is simplest to consider a specific example.

Suppose that a 25-dB modified Taylor[1] distribution is selected for an aperture design. This distribution produces a 25-dB first sidelobe level, with approximately a sin u/u falloff for higher order sidelobes. In this instance, the normalized aperture distribution is specifically

$$f(z) = \frac{1}{2\pi} J_o\left(j\ 1.02292\pi\sqrt{1 - 4z^2}\right)$$

$$-0.5 \leq z \leq 0.5$$

where J_o is the zero-order Bessel function of the first kind. Figure 3-6 shows $f(z)$ and $[f(z)]^2$. With Dion's[2] approach for the traveling-wave array,

$$g(z) = \frac{P(z)}{P_o(z)} \tag{9}$$

where $P(z)$ is the power radiated per unit length, $P_o(z)$ is the available power in the waveguide, and $g(z)$ is the normalized conductance per unit length at a distance z from the center of the array. For a case more general than Dion's, in which waveguide loss may have to be considered, Equation (9) takes the form

$$Lg(z) = \frac{[f(z)]^2\ e^{2\alpha Lz}}{\left[\frac{e^{-2\alpha L}}{e^{-2\alpha L} - r}\right] \int_{-0.5}^{0.5} [f(w)]^2\ e^{2\alpha Lw} dw - \int_{-0.5}^{z} [f(w)]^2\ e^{2\alpha Lw}\ dw} \tag{10}$$

where α is the waveguide wall loss constant in nepers per unit length, L is the overall array length, and r is the fraction of input power absorbed by

25 dB MODIFIED TAYLOR DISTRIBUTION (AMPLITUDE & POWER)

FIGURE 3-6

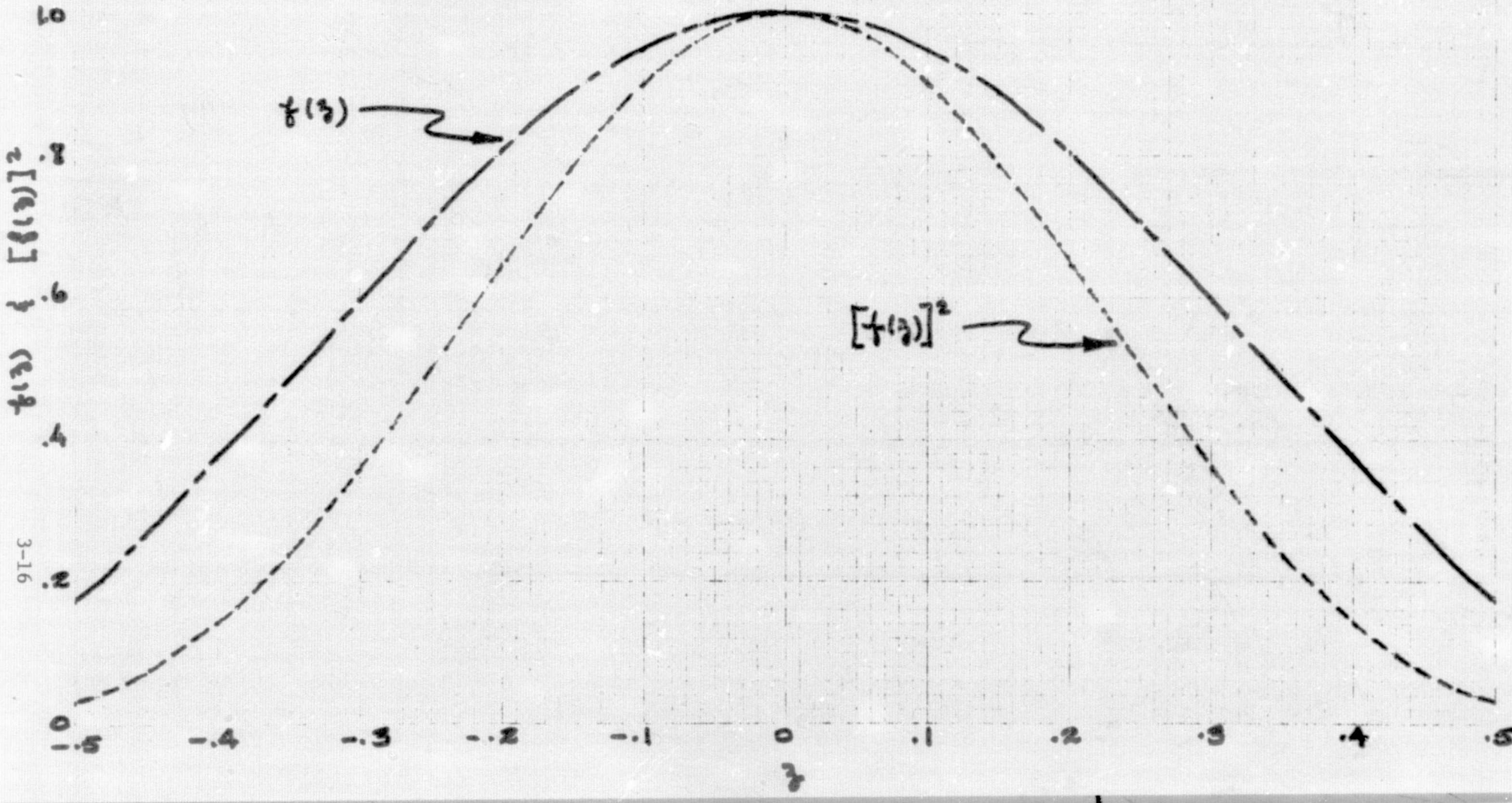

the load. When α can be considered negligible, the function Lg(z) is universal and applied to arrays of any length as long as a continuous distribution is appropriate. This universality is not the case when loss must be included.

Equation (10) is plotted for the three cases shown in Figure 3-7. All assume 5-percent power to the load. The 5-meter and 18-meter cases further assume a loss factor associated with standard aluminum X-band waveguide of 1.5581×10^{-2} nepers per meter at 10 GHz.

Equation (10) and the curves of Figure 3-7 present conductance normalized to the overall array length. For these curves to be utilized in computation of actual slot conductance values, the value Lg(x) associated with a particular slot in the aperture must be located and then divided by the total number of slots in the array. Clearly, very small conductance values must result when long arrays are considered. Table 3-I shows minimum and maximum normalized conductance values, with the lossless curve, for 1-percent and 5-percent power to the load.

TABLE 3-I. MINIMUM AND MAXIMUM NORMALIZED SLOT CONDUCTANCES

	5-m Array		18-m Array	
r	g_{min}	g_{max}	g_{min}	g_{max}
0.01	1.738×10^{-4}	3.354×10^{-2}	4.831×10^{-5}	9.322×10^{-3}
0.05	1.668×10^{-4}	1.903×10^{-2}	4.636×10^{-5}	5.29×10^{-3}

Two questions are suggested from the values in Table 3-I: first, are these conductance values practically realizable, and second, are slot-to-slot conductance changes so small that machining tolerances might cause serious inaccuracy in the desired conductance characteristic? Recent work suggests that short, non-resonant, slots can be used to achieve very small conductances and that there is good correlation between experiment and theory.[3,4] Independent development of this theory has resulted in the

NORMALIZED CONDUCTANCE
MRF 5M & 18M. ARRAYS
25 dB MODIFIED TAYLOR DISTRIBUTION
STD ALUMINUM X-BAND WAVEGUIDE
WALL LOSS
5% POWER TO LOAD

FIGURE 3-7

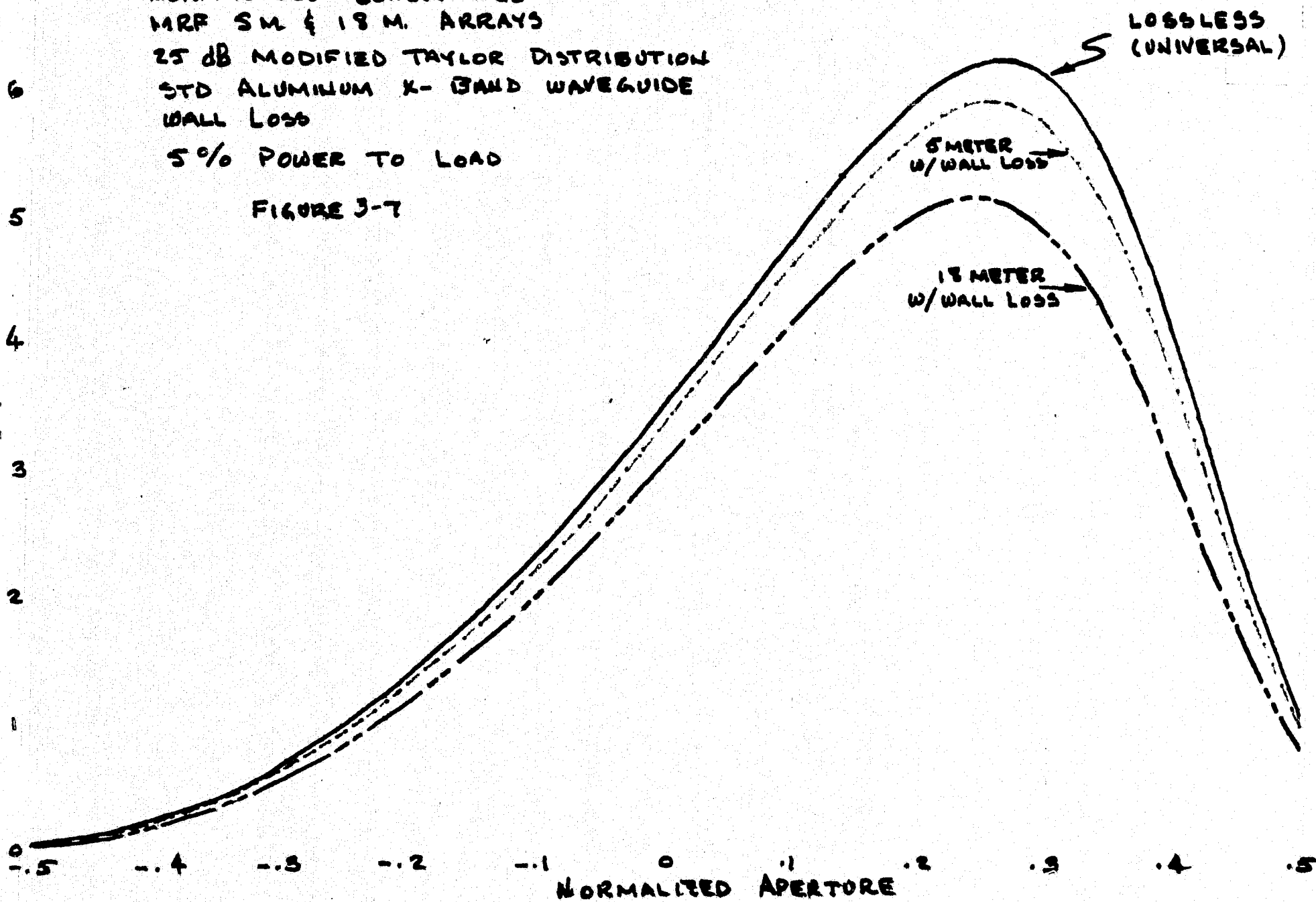

admittance data shown by Figures 3-8 to 3-11. Note that the conductance limits from Table 3-I are indicated in the margins of Figures 3-8 and 3-10. There appears to be a reasonable range of slot offsets and lengths over which the indicated conductances can be obtained.

The sensitivity of conductance as a function of offset and length is of particular interest. From Figure 3-8,

$$g(0.420,\ \ell) \simeq 5.98 \times 10^{-7}\ \ 10^{10.0571\ell}$$

$$g(0.240,\ \ell) \simeq 3.63 \times 10^{-7}\ \ 10^{10\ell}.$$

These characteristics indicate that a 0.001-inch error in slot length will produce a one-percent change in slot conductance, while a 0.003-inch error in offset produces approximately a 1-percent change. Similar results apply for Figure 3-9. If random, an error of this magnitude will likely have negligible impact on performance. This statement is not true for systematic errors. Great care must be taken to avoid monotonic conductance errors and those that cause significant ripple in the aperture distribution.

Table 3-II presents minimum and maximum reflection coefficients associated with the r = 0.05 conductances of Table 3-I. An 0.420-inch offset from Figures 3-8 to 3-11 was used for this purpose. Each admittance was assumed to be terminated by a match load. Related transmission coefficients are also shown. These figures are within the limits normally judged acceptable for traveling-wave arrays. However, the maximum reflection coefficient for the 5-meter array indicates that some extra care might be advisable for this region of the aperture.

TABLE 3-II. REFLECTION AND TRANSMISSION COEFFICIENTS FOR 5-METER AND 18-METER ARRAYS

Array	Conductance	Susceptance	Slot Length, inches	Reflection Coefficient	Transmission Coefficient
5m	0.0001668	0.0185	0.244	0.009 $\angle$-91°	1 $\angle$.5°
	0.001903	0.142	0.449	0.0707 $\angle$-94.8°	0.997 $\angle$-4°
18m	0.00004636	0.0115	0.203	0.006 $\angle$-90.5°	1 $\angle$-.3°
	0.00529	0.079	0.392	0.0395 $\angle$-96°	0.998 $\angle$-2.3°
	5% Power to load Offset - 0.420 inch				

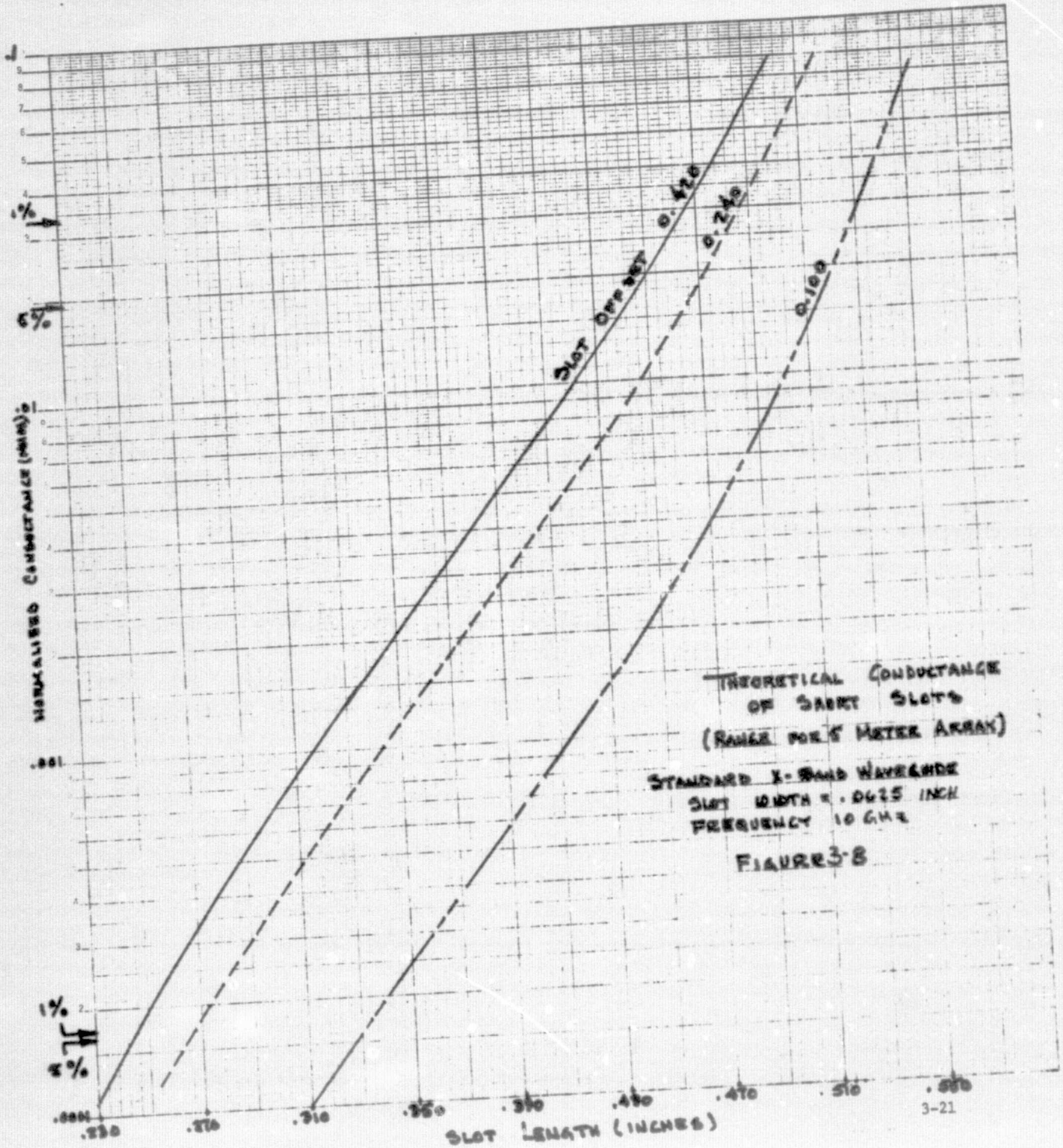

THEORETICAL CONDUCTANCE OF SHUNT SLOTS (RANGE FOR 5 METER ARRAY)

STANDARD X-BAND WAVEGUIDE
SLOT WIDTH = .0625 INCH
FREQUENCY 10 GHz

FIGURE 3-8

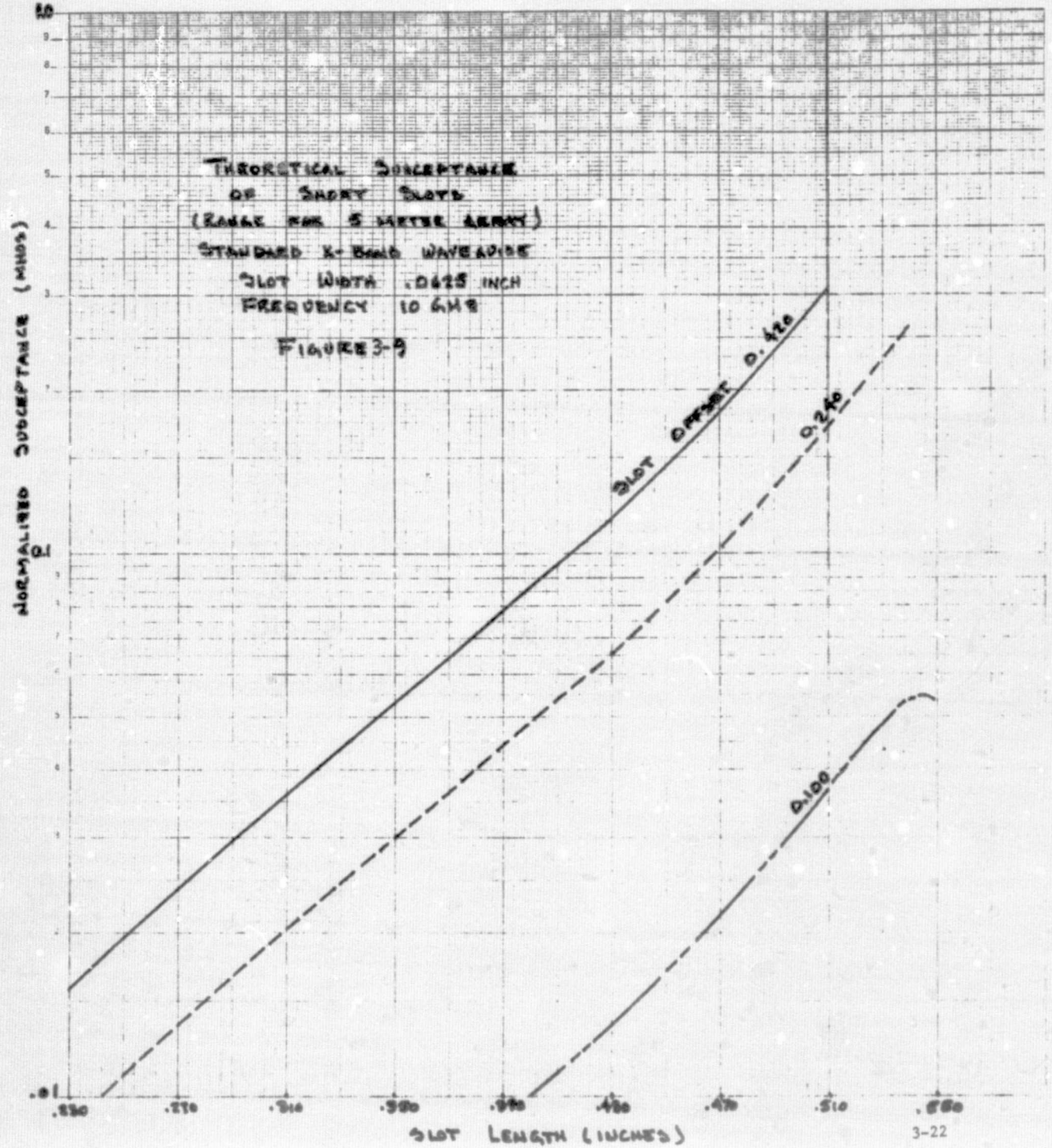
THEORETICAL SUSCEPTANCE
OF SHORT SLOTS
(RANGE FOR 5 WAVEGUIDE ARRAY)
STANDARD X-BAND WAVEGUIDE
SLOT WIDTH .0625 INCH
FREQUENCY 10 GHz
NORMALIZED SUSCEPTANCE (MHOS)
SLOT OFFSET 0.420
0.240
0.100
SLOT LENGTH (INCHES)

FIGURE 3-9

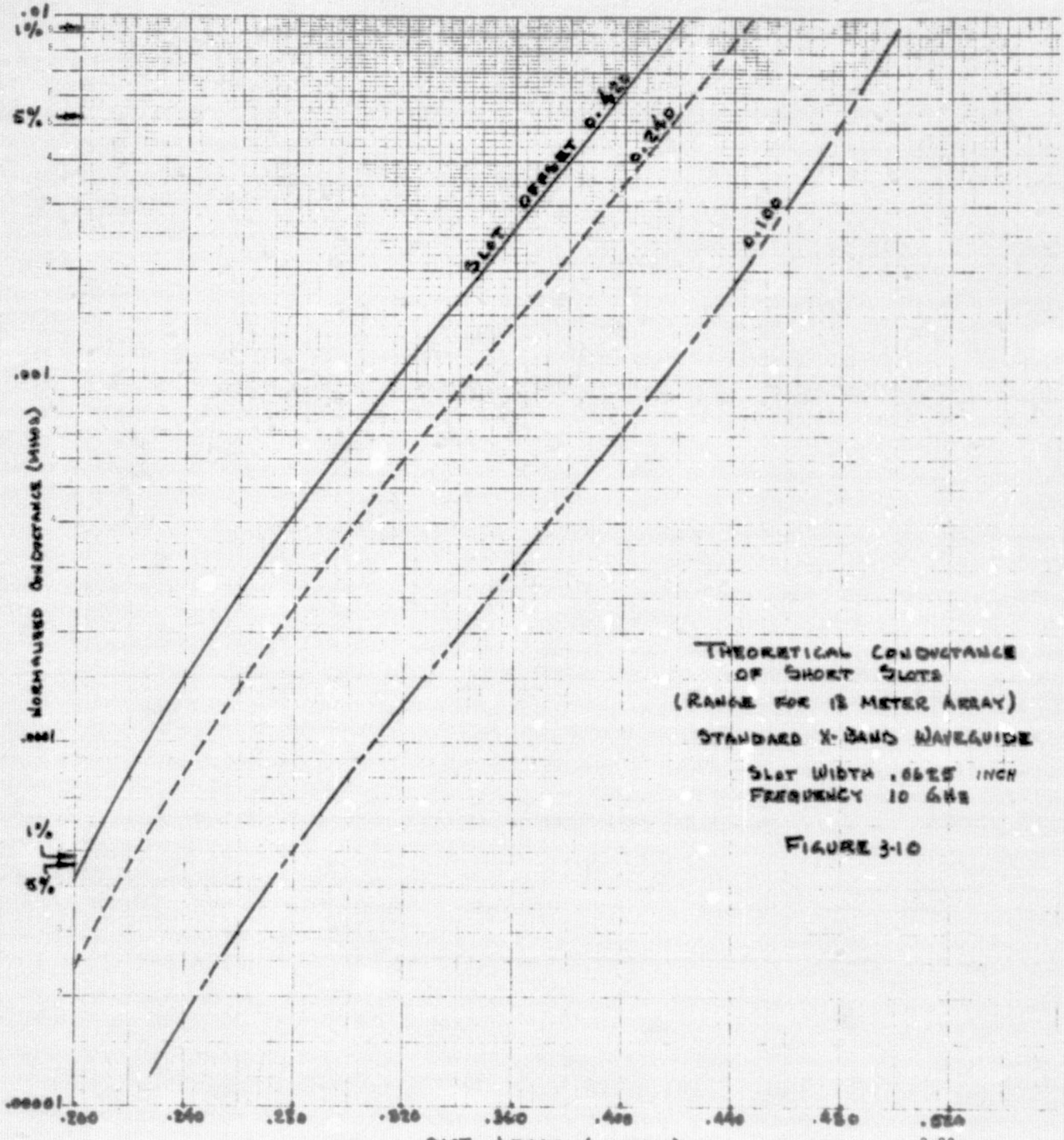

THEORETICAL CONDUCTANCE
OF SHORT SLOTS
(RANGE FOR 13 METER ARRAY)
STANDARD X-BAND WAVEGUIDE
SLOT WIDTH .0625 INCH
FREQUENCY 10 GHz

FIGURE 3-10

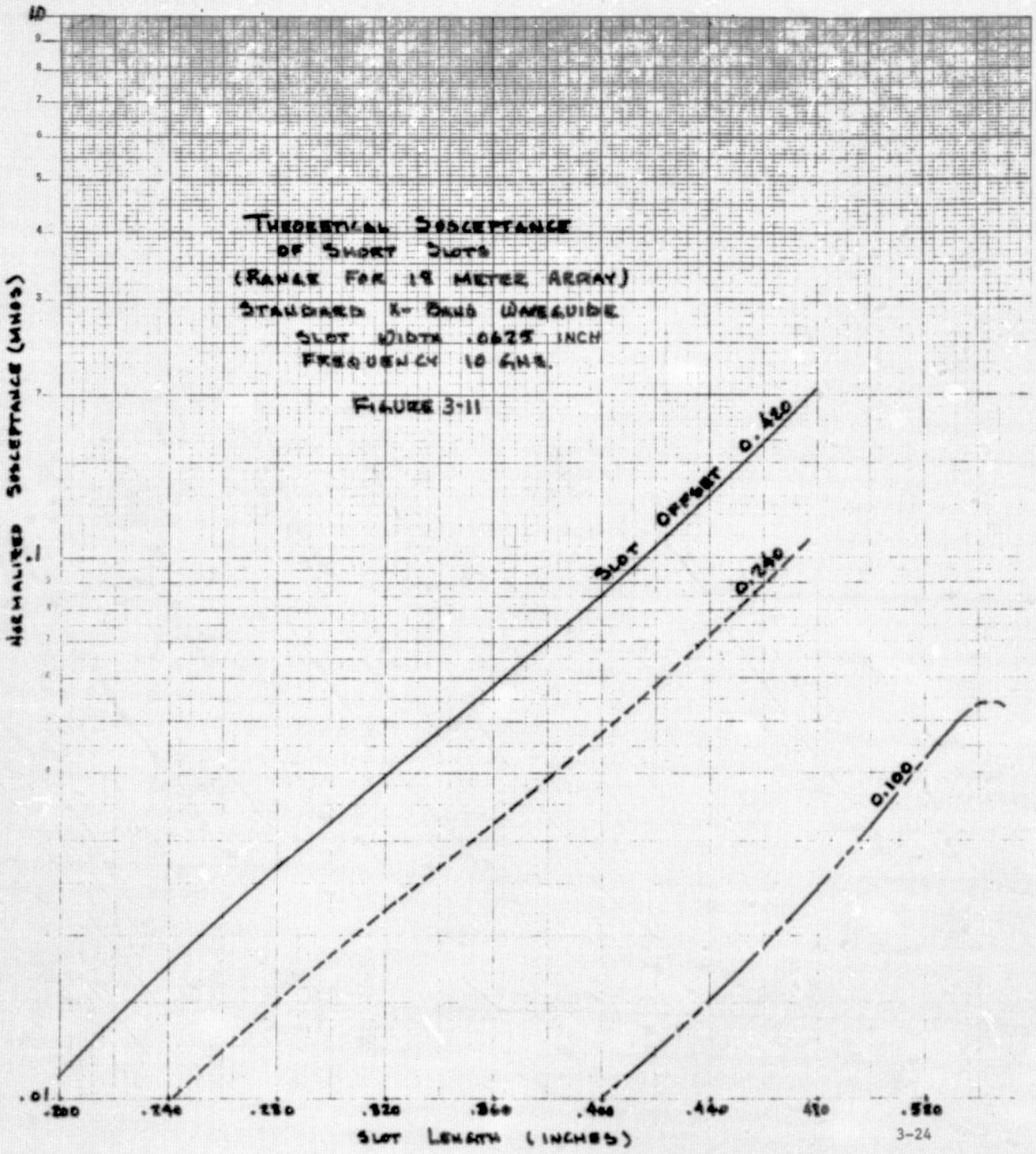
THEORETICAL SUSCEPTANCE
OF SHORT SLOTS
(RANGE FOR 19 METER ARRAY)
STANDARD X- BAND WAVEGUIDE
SLOT WIDTH .0625 INCH
FREQUENCY 10 GHz.
NORMALIZED SUSCEPTANCE (MHOS)
SLOT OFFSET 0.420
0.240
0.100
.01
.200
.240
.280
.320
.360
.400
.440
.480
.520
SLOT LENGTH (INCHES)

FIGURE 3-11

4.0 STABILITY REQUIREMENTS

For the transmitting antenna to illuminate a circle formed by the intersection of a cone and a plane or spherical cap or for the receiving antenna beams to lie on such a cone, the axis of the cone or of the array must be held perpendicular to the plane or along the radius, i.e., the local vertical of the spherical cap that approximates the earth below the shuttle. If the array axis is tilted relative to the vertical, then the interception of the cone of radiation and the earth is no longer circular and the range to the intercept with the earth will vary with azimuth angle. Interference of the ground return with returns from the atmosphere at lower levels will result as well as interference between returns in different range resolution cells. If, for example, the tilt of the array axis occurs in the plane perpendicular to the flight vector, as it would with roll of the Shuttle, the angular change to produce a one kilometer difference in range to level ground from an altitude of 400 kilometers is 0.1 degree. The implication is that stabilization of the antenna independent of the Shuttle may be required. A relatively straightforward method by which such stabilization can be accomplished, given an appropriate directional reference, is indicated in Section 2. One possible method of providing the appropriate reference is to derive the perpendicular to the ground by range measurement at several beam positions.

5.0 ANTENNA SPECIFICATION

The receiving portion of the meteorological radar antenna, as contemplated, operates in an unconventional way in that no azimuth pattern is formed in the physical equipment that would ordinarily constitute the antenna. Rather, the output of each of the individual longitudinal traveling-wave arrays is delivered to a receiver, and the azimuthal response is determined in subsequent processing of the multiple signals from the elements. As a consequence, the required antenna performance, as a separate piece of hardware, cannot be entirely specified practicably in the conventional way. The overall performance is that determined by the combination of the microwave components, the system, and the processing portion. For the processor formation of the overall azimuthal response, two conditions must be met:

1. The elevation responses of the individual elements in the presence of the others, when terminated by the receivers, i.e., the pattern in any plane passing through the antenna longitudinal axis, need to be alike within some tolerance.
2. The azimuthal response of the elements also must be the same within some tolerance.

Similarity of response implies both amplitude and phase and can be considered as expressed by a transfer function from the radiation field at a point outside the aperture, not necessarily in the conventional far zone, to the signal at the element output.

The far-field patterns of the active elements must meet some conventional requirements in that the peaks of the pattern must lie at a specified angle within some tolerance, but since these responses are combined in the processor, it is not clear at this juncture how much the angular responses of the individual elements can be permitted to vary in either direction. Both an overall response error budget and a statistical analysis,

which might best be performed by the Monte Carlo technique, are required before specification can be accomplished.

REFERENCES

1. Thomas T. Taylor, One Parameter Family of Line Sources Producing Sin u/u Patterns, Tech. Memo No. 324, Hughes Aircraft Co., September 1953.

2. Andre Dion, "Nonresonant Slotted Arrays," IRE Trans. on Antennas and Propagation, Vol. AP-6, No. 4, pp. 360-365, October 1958.

3. M. E. Armstrong and N. G. Alexopoulos, "On the Design of a Circularly Polarized Waveguide Narrow Wall Linear Array," IEEE Trans. on Antennas and Propagation, Vol. AP-23, No. 2, pp. 244-250, March 1975.

4. Arthur A. Oliver, "The Impedance Properties of Narrow Radiating Slots in the Broad Face of Rectangular Waveguide," IRE Trans. on Antennas and Propagation, Vol. AP-5, No. 1, pp. 4-20, January 1957.

APPENDIX
INTERELEMENT PHASE SHIFT FOR γ = 90 DEGREES

1. Select σ = 45 degrees (arbitrary)

Then $\frac{\lambda_o}{\lambda_g} = \frac{\sqrt{2}}{2}$

This forces the 'a' dimension because $\frac{\lambda_o}{\lambda_g} = \sqrt{1 - \left(\frac{\lambda_o}{2a}\right)^2}$

$$\frac{\lambda_o}{2a} = \sqrt{1 - \left(\frac{\lambda_o}{\lambda_g}\right)^2} \qquad a = \frac{\lambda_o}{2\sqrt{1 - \left(\frac{\lambda_o}{\lambda_g}\right)^2}}$$

Therefore, if zero wall thickness is assumed, the arbitrary choice of σ dictates d_x directly

In this case $a = \frac{\lambda_o}{\sqrt{2}} = d_x = 0.835$ inch

2. Select d_y = 0.691 inch (arbitary)

Now $\lambda_g = \frac{\lambda_o}{\cos\sigma} = \sqrt{2}\,\lambda_o$

so that $\psi_y = \frac{2\pi}{\sqrt{2}\lambda_o}(0.691) = \underline{149}$ degrees

Therefore, the arbitrary choice of σ and d_y dictates both a and ψ_y.

3. Now

$$\frac{\psi_x \lambda_o}{2\pi d_x} = \sin\sigma \sin\gamma$$

but d_x and σ are already defined.

Therefore,

$$\frac{\psi_x \lambda_o}{2\pi} = 0.835 \frac{\sqrt{2}}{2} \sin\gamma = 0.5904 \sin\gamma$$

$$\sin\gamma = \frac{1.6937\ \psi_x \lambda_o}{2\pi}$$

If it is desired that γ = 90 degrees for a σ selected to be 45 degrees, then

$$\psi_x = \frac{360}{1.6937\ \lambda_o} = 180 \text{ degrees}$$

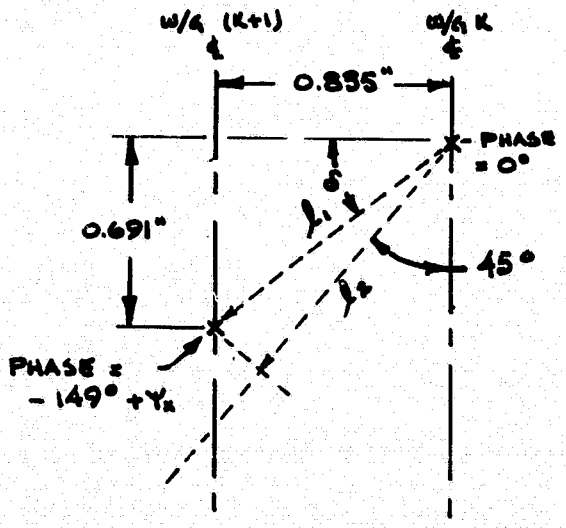

$$\delta = \tan^{-1}\frac{.691}{.835} = \tan^{-1} .827$$

$$\delta = 39.609°$$

$$\ell_1 = 1.0838$$

$$\ell_2 = \ell_1 \cos(45 - \delta)$$

$$= 1.0838 \cos(5.391°)$$

$$\ell_2 = 1.079" = .9142\ \lambda_o$$

$$k\ell_2 = 329.107 \text{ degrees}$$

Therefore, ψ_x must equal 180 degrees in order to fire in-phase at $\gamma = 90°$, $\sigma = 45°$.

If d_y had been selected as 0.500 inch, then

$$\psi_y = \frac{2\pi}{\sqrt{2}\ \lambda o}\ (0.5) = 107.84 \text{ degrees}$$

$$\ell_1 = 0.97325$$

$$\delta = 30.91 \text{ degrees}$$

$$\ell_2 = 0.97325 \cos 14.09° = 0.94397 = 0.8\ \lambda_o$$

$$k\ell_2 = 287.92 \text{ degrees}$$

and, again, ψ_x must equal 180 degrees.